Simulated Surface Potentials at the Vapor-Water Interface for the KCl Aqueous Electrolyte Solution

Collin D. Wick and Liem X. Dang

Chemical Sciences Division,

Pacific Northwest National Laboratory,

Richland, WA 99352

and

Pavel Jungwirth

Institute of Organic Chemistry and Biochemistry, Academy of Sciences of the Czech Republic, and Center for Complex Molecular Systems and Biomolecules, Flemingovo nám. 2, 16610 Prague 6, Czech Republic

Abstract

Classical molecular dynamics simulations with polarizable potential models were carried out to quantitatively determine the effects of KCl salt concentrations on the electrostatic surface potentials of the vapor-liquid interface of water. To the best of our knowledge, the present work is the first calculation of the aqueous electrolyte surface potentials. Results showed that increased salt concentration enhanced the electrostatic surface potentials, in agreement with the corresponding experimental measurements. Furthermore, the decomposition of the potential drop into contributions due to static charges and induced dipoles showed a very strong effect (an increase of ~1V per 1M) due to the double layers formed by KCl. However, this was mostly negated by the negative contribution from induced dipoles, resulting in a relatively small overall increase (~0.05V per 1M) with increased salt concentration.

I. INTRODUCTION

The interfaces between an aqueous solution and its vapor have been widely studied due to their importance for biological, environmental, and atmospheric chemistry.[1] The measurement of surface potential has long been a technique to determine the interfacial water orientation and ion distribution at vapor-liquid interfaces. The surface potential is defined as the difference in electrical potential between a neutral aqueous liquid and its coexisting vapor phase. The direct experimental determination of the surface potential remains a challenge. The surface potential across the interface between a vapor and neat water being a point of contention, with surface potential measurements not always agreeing on sign.[2,3] However, the facts that the surface potential increases with the addition of alkali halide salts,[4] and that it decreases with increased temperature for pure water,[5] are currently accepted.

Considerable progress has been made during the past decade in utilizing computational techniques to understand the equilibrium properties (i.e., orientational structure, surface potentials, surface tensions, etc.) of the vapor-liquid interface of water.[6] In particular, many of the efforts in this area of research have focused on computing the surface potential, χ, using molecular simulation techniques. Pratt and co-workers are pioneering in this field and have computed χ=–130±50 mV for the TIP4P[7] water model.[8] Recently different calculations by Zakharov et al. have shown a significantly higher in magnitude value of χ for this model (i.e., –550±4 mV).[9] Sokhan and Tildesley have conducted detailed studies of equilibrium properties including the temperature dependence of the vapor-liquid interface of water using the SPC/E water model.[10] They reported a value of –550 mV for χ. Most of the simulation work on surface properties to date has used pairwise additive models, which do not include explicit polarization. While similar results for pairwise and many-body potentials were

found across the vapor-liquid interface of neat water at 298 K,[11] the effects for systems with electrolyte salts are less understood.

The primary aim of the current study is to determine the effect of polarization on the surface potential across the vapor-liquid interface of aqueous systems with the addition of electrolyte salts. This paper is organized as follows. The polarizable model potentials and the simulation methods are summarized in Section II. The electric field and surface potential results are presented and discussed in Section III. Our conclusions and discussion of future research directions are presented in Section IV.

II. MOLECULAR MODELS AND SIMULATION METHODS

The water model used in this study was the polarizable Dang-Chang model, which has four sites, including an oxygen site, two hydrogens, and an *m* site located along the bisector of the oxygen-hydrogen bonds.[12] The ions were modeled with a single site polarizable potential,[12,13] which was parameterized to reproduce *ab initio* ion-water interactions, experimental solvation enthalpies, and structural properties of ion solvation in water. All models included interactions consisting of Lennard-Jones, Coulombic, plus a polarizable term to describe many-body effects. Many-body effects have been found to be essential to understand salt concentrations at the vapor-water interface.[14] The details of the potential models, including the method for computing induction effects are reported in our previous work.[12,13] A potential truncation of 9 Å was enforced with analytical tail corrections for the Lennard-Jones interactions. For electrostatic interactions, the particle mesh Ewald summation technique was used. Water molecules were kept rigid utilizing the SHAKE algorithm.[15] Simulations were performed for pure water, 1M and 2M KCl aqueous solutions at 298 K. For each system, 1000 water molecules were included along with 0, 18 and 36 ion pairs for the pure, 1M and 2M systems, respectively. All systems were placed in periodic boxes elongated in the *z* direction creating two vapor-liquid interfaces, and periodic liquid

along the x and y directions. On average, the liquid slab dimensions were twice as long in the z direction as the x and y, and the Berendsen thermostat was used to control the temperature.[16]

The atomic approach was used to determine the effects of the atomic partial charge distributions and induced dipole moments on the electrostatic potential difference across the vapor-liquid interface. The electric potential difference across the interface, $\Delta\phi_q(z)$, is defined as[8,10]

$$\Delta\phi_q(z) = \phi_q(z) - \phi_q(z_0) = \frac{1}{\varepsilon_0}\int_{z_0}^{z} \mathrm{E}_z(z')\mathrm{d}z' \tag{1}$$

Where z_0 denotes a reference point in the charge-free (vapor) region and $\mathrm{E}_z(z)$ is the electric field derived from point charges as a function of z across the vapor-liquid interface. $\mathrm{E}_z(z)$ is calculated by integrating the charge distribution along the z axis from the vapor to the liquid phase

$$\mathrm{E}_z(z) = \frac{1}{\varepsilon_0}\int_{z_0}^{z} \left\langle \rho_q(z') \right\rangle \mathrm{d}z' \tag{2}$$

where $<\rho_q(z)>$ is the ensemble averaged charge density profile which was evaluated in slabs of 0.25 Å thickness along the z direction. The electrostatic potential due to the induced dipole moment associated with each molecule as a result of the polarizability can be computed as follows

$$\Delta\phi_\mu^{\mathrm{ind}}(z) = \phi_\mu^{\mathrm{ind}}(z) - \phi_\mu^{\mathrm{ind}}(z_0) = \frac{1}{\varepsilon_0}\int_{z_0}^{z} \left\langle \rho_\mu^{\mathrm{ind}}(z') \right\rangle \mathrm{d}z' \tag{3}$$

The density profile of the induced dipole moments normal to the interface, $<\rho_\mu^{\mathrm{ind}}(z)>$, was evaluated as the average of the normal (z) component of the induced dipole moments in the liquid using slabs of 0.25 Å thickness along the z axis. By adding the contributions from the partial charges and induced dipole moments, the total surface

potential can be obtained. The data were collected over 1 ns molecular dynamics simulation time after extensive equilibration.

III. RESULTS AND DISCUSSION

The total electric potential as a function of position for all systems studied are given in FIG. 1, and the decomposition of the surface potentials into contributions from static charges and induced dipoles at 298 K for pure water, 1M KCl, and 2M KCl are given in FIG.2. Table 1 gives the corresponding average values of the total surface potential and its contributions from static charges and induced dipoles in the bulk liquid (>15 Å from the Gibbs dividing surface of water) for all systems studied. The value obtained in the current study for water (-480 mV) is consistent with that of a previous study of the surface potential of the Dang-Chang water,[11] and the most recent values calculated for the non-polarizable TIP4P and SPC/E water models.[9,10] We calculate the probability distributions for the angle between the water C_{2v} molecular axis and the z-axis as a function of the z coordinate. The results clearly indicate the presence of a preferred orientational order of water molecules near the interface. As the water approaches the interface, the probability of the angle between water molecular axis and the interface normal around 90^o increases significantly, meaning that the water permanent dipoles prefer to lie parallel to the interface.

Experimental studies have argued that the water surface potential should be slightly positive,[3,5] in disagreement with our simulation results and other computational studies. The claim was that as the temperature increases, the magnitude of the surface potential should decrease up to its critical point, where it would be zero. On the other hand, Tildesley and co-workers have demonstrated that the temperature dependence of the surface potential utilizing the SPC/E water model to decrease with increasing temperature (250-350 K) and to increase with increasing temperature (350-550 K).[10]

The addition of KCl salt increases the surface potential, in agreement with experimental observations.[4] The decomposition of the surface potential into contributions from static charges and induced dipoles provides interesting insight. The static potential shows a significant double layer effect due to the separation of KCl at the interface. The density profiles for the 1M salt solutions given in FIG. 3 confirm this, by showing the higher anion concentration near the Gibbs dividing surface. Also, it shows an increase in K^+ density between –5 and –7.5 Å from the Gibbs dividing surface, just next to the region where anion density is greater than cation density. This double layer creates a dipole at the surface pointing towards the gas phase, which contributes negatively to the electric field and a positively to the surface potential from the vapor to the liquid.

The induced dipole contribution to the surface potential is strongly negative for all salt solutions. These dipoles are induced by anisotropic hydrogen bonding patterns between waters and anions at the interface. Anions at the surface have a majority of their hydrogen bonds directed towards the liquid bulk. For non-polarizable anions, this would be expected to reduce their propensity at the interface. However, if polarizability is allowed, a dipole can be induced pointing towards the bulk liquid, strengthening these hydrogen bonds and increasing their propensity to be at the interface.[17] How much propensity these anions have for the vapor-water interface is dependent on the strength of polarization and their atomic size, with larger, more polarizable anions having higher concentrations at the interface.[18] These induced dipoles result in a negative contribution to the total potential drop, significantly counterbalancing the effect of the charge double layer from the KCl densities on the total surface potential. Overall, this leads to a small increase in the potential drop (10-20 mV per 1 M) for the addition of salt to water.

Another interesting feature is present for the KCl solutions. KCl shows only small differences in the static and induced dipole contributions to the total surface

potential between the 1M and 2M KCl systems as seen in Table 1 and FIG. 2. While the change in total surface potential between pure water and 1M KCl are of similar magnitude as between 1M and 2M KCl, the changes in the decomposed values are very significant between pure water and 1M KCl, but quite small between 1M and 2M KCl. This gives evidence that the magnitude of charge separation has hit a plateau, but the experimental trend of linear increases in total surface potential as a function of salt concentration is still observed.[4] The origin of this plateau appears to be the result of the depth of the interfacial region, as defined by the region where the decomposed electrostatic potential changes as a function of *z*. The 1M KCl solution does not show leveling off of the electrostatic potential until around 15 Å from the Gibbs dividing surface, but the 2M KCl solution levels off around 7.5 Å. While the 2M KCl solution shows a sharper change of electrostatic potential near the Gibbs dividing surface than 1M KCl, the longer length of the effect for the 1M KCl solution counterbalances this, leading to similar totals in decomposed surface potentials.

IV. CONCLUSIONS

Molecular dynamics simulations with polarizable potentials were carried out to determine the effect of KCl salt concentration on the surface potential across a vapor-water interface. The results compared well with experimental observations and previous simulations of both polarizable and non-polarizable models. Decomposing the surface potential into contributions from static charge and induced dipole contributions showed that the interfacial distribution of static charges is strongly affected by the introduction of salt ions, but the induced dipole contribution is opposite and nearly equal, leading to a small increase in total surface potential. In our opinion, the result from these calculations is interesting, if one only focused on the change in total surface potential, it would *not* lead to an assumption of a very strong ion double layer. Due to the ability to decompose the surface potential in these calculations, it is

observed that there can simultaneously be strong ion double layering and relatively small changes in total potential drop due to the effect of the strong induced dipoles of interfacial anions.

ACKNOWLEDGEMENTS

This work was supported by the Office of Basic Energy Sciences of the Department of Energy, in part by the Chemical Sciences program and in part by the Engineering and Geosciences Division. The Pacific Northwest National Laboratory is operated by Battelle for the U.S. Department of Energy. The funding of the Center for Biomolecules and Complex Molecular Systems is provided by the Ministry of Education of the Czech Republic under the project number LC512. The work performed at the Institute of Organic Chemistry and Biochemistry of the Academy of Sciences of the Czech Republic was a part of the research project Z40550506 and via the NSF-funded Environmental Molecular Science Institute (grants CHE 0431512 and 0209719) is gratefully acknowledged.

Figure Captions

FIG 1. Electrostatic potential as a function of distance from the Gibbs dividing surface of water across the vapor-liquid interface.

FIG 2. Decomposition of the electrostatic potentials shown in FIG. 1 into contributions from static charges (solid lines) and induced dipoles (dashed lines).

FIG 3. Density profiles of K^+ and Cl^- for the 1M and 2M KCl aqueous solutions.

Table 1: The computed surface potentials and corresponding compoments

System	Total χ(V)	Charge χ(V)	Induced Dipole χ(V)
Water (T=298 K)	–0.480±0.002	–0.276±0.001	–0.205±0.001
1 M KCl	–0.445±0.002	0.621±0.006	–1.066±0.005
2 M KCl	–0.408±0.003	0.608±0.011	–1.016±0.009

References

[1] A. Morita and J. T. Hynes, Journal Of Physical Chemistry B **106** (3), 673 (2002).

[2] D. D. Eley and E. M. G., Trans. Faraday Soc. **34**, 1093 (1938); M. Saloman, Journal Of Physical Chemistry **74**, 2519 (1970).

[3] M. Paluch, Advances In Colloid And Interface Science **84** (1-3), 27 (2000).

[4] J. E. B. Randles, Phys. Chem. Liq. **7**, 107 (1977).

[5] J. R. Farrell and P. McTigue, Journal Of Electroanalytical Chemistry **163** (1-2), 129 (1984).

[6] P. Jungwirth and D. J. Tobias, Chemical Reviews **106** (4), 1259 (2006); T. M. Chang and L. X. Dang, Chemical Reviews **106** (4), 1305 (2006).

[7] W. L. Jorgensen, J. Chandrasekhar, J. D. Madura, R. W. Impey, and M. L. Klein, Journal Of Chemical Physics **79** (2), 926 (1983).

[8] M. A. Wilson, A. Pohorille, and L. R. Pratt, Journal Of Chemical Physics **88** (5), 3281 (1988).

[9] V. V. Zakharov, E. N. Brodskaya, and A. Laaksonen, Journal Of Chemical Physics **107** (24), 10675 (1997).

[10] V. P. Sokhan and D. J. Tildesley, Molecular Physics **92** (4), 625 (1997).

[11] L. X. Dang and T. M. Chang, Journal Of Physical Chemistry B **106** (2), 235 (2002).

[12] L. X. Dang and T. M. Chang, Journal Of Chemical Physics **106** (19), 8149 (1997).

[13] L. X. Dang, Journal Of Physical Chemistry B **106** (40), 10388 (2002).

[14] P. Jungwirth and D. J. Tobias, Journal Of Physical Chemistry B **106** (25), 6361 (2002).

[15] J. P. Ryckaert, G. Ciccotti, and H. J. C. Berendsen, Journal Of Computational Physics **23** (3), 327 (1977).

[16] H. J. C. Berendsen, J. P. M. Postma, W. F. Vangunsteren, A. Dinola, and J. R. Haak, Journal Of Chemical Physics **81** (8), 3684 (1984).

[17] C. D. Wick and L. X. Dang, Journal Of Physical Chemistry B **110** (13), 6824 (2006).

[18] L. Vrbka, M. Mucha, B. Minofar, P. Jungwirth, E. C. Brown, and D. J. Tobias, Current Opinion In Colloid & Interface Science **9** (1-2), 67 (2004).

FIG. 1

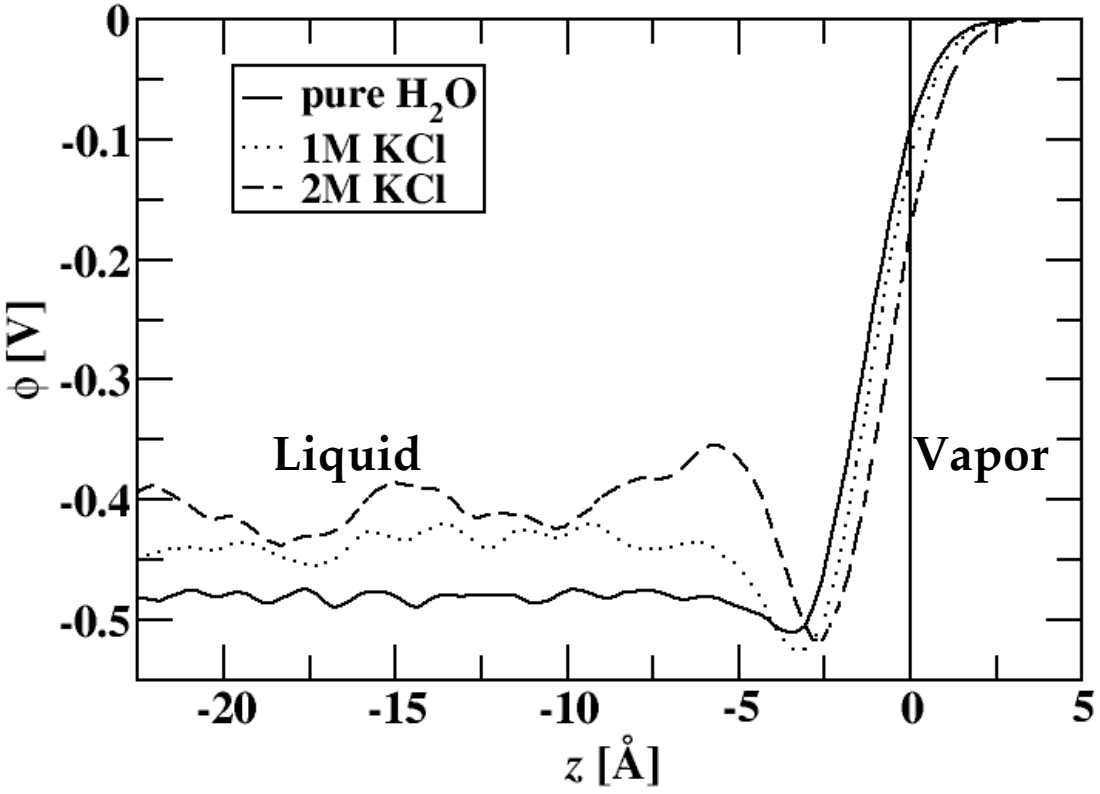
pure H_2O
1M KCl
2M KCl
Liquid
Vapor
ϕ [V]
z [Å]
0
-0.1
-0.2
-0.3
-0.4
-0.5
-20
-15
-10
-5
0
5

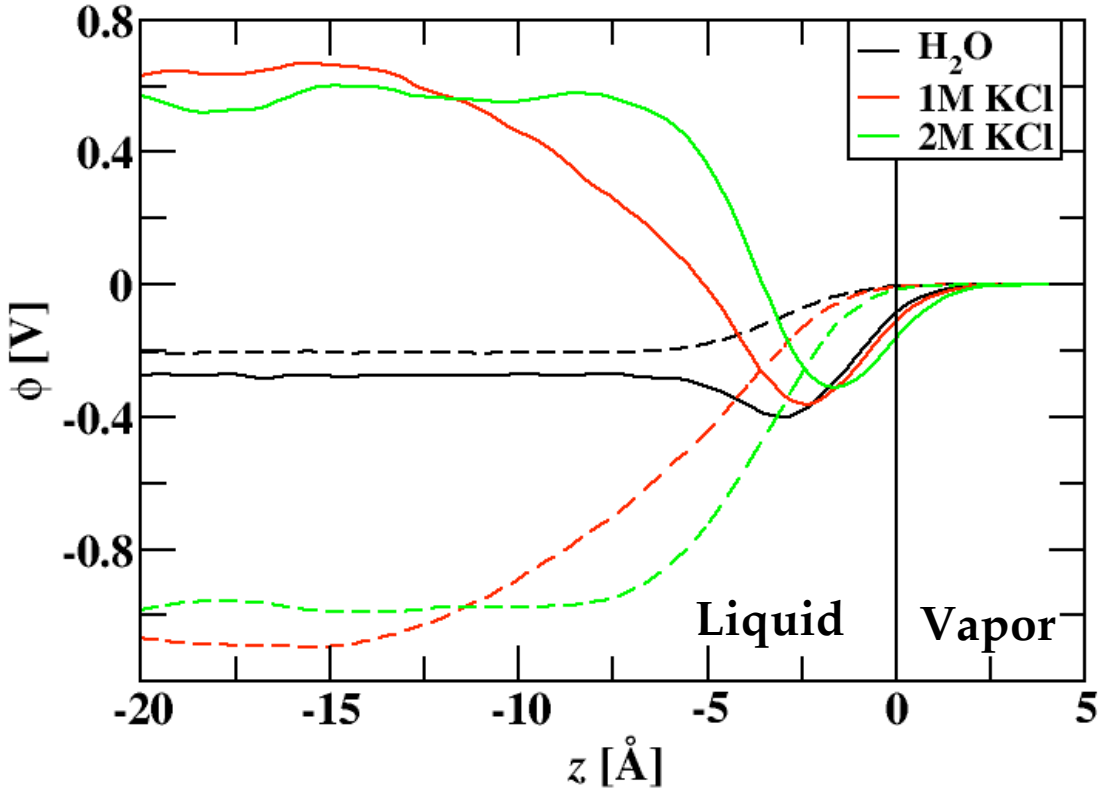

FIG. 2.

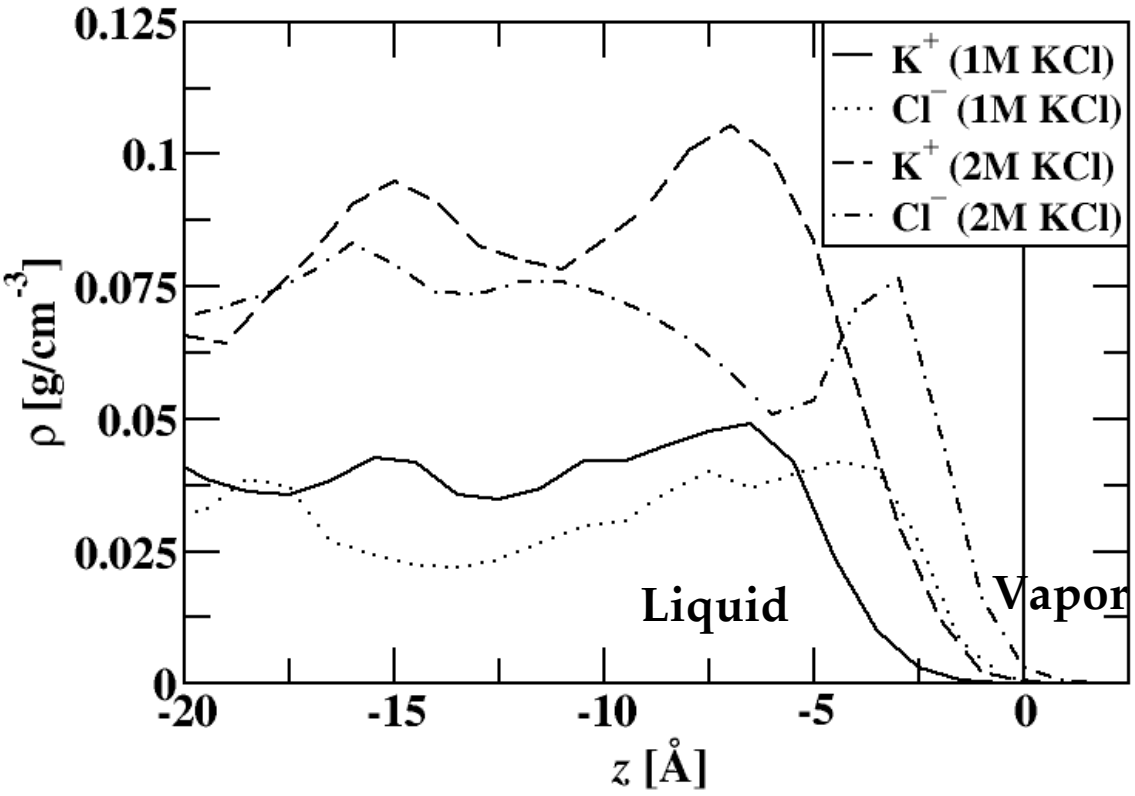
0.125
0.1
0.075
0.05
0.025
0
ρ [g/cm^-3]
-20
-15
-10
-5
0
z [Å]
K+ (1M KCl)
Cl− (1M KCl)
K+ (2M KCl)
Cl− (2M KCl)
Liquid
Vapor

FIG. 3.